Deytec Technical Report No. 2009-03

Validation of the CFAST and FDS Fire Models for Cable Exposure to Pool Fires in a Trench

Deytec, Inc.

Nuclear Engineering Services

Validation of the CFAST and FDS Fire Models for Cable Exposure to Pool Fires in a Trench

March 2009

Prepared by
Dr. Monideep K. Dey

HC-64, Box 100-27
Yellow Spring, WV 26865
USA

Deytec, Inc.
Nuclear Engineering Services

Abstract

The analysis presented in this report was conducted for Benchmark Exercise # 5 in the International Collaborative Fire Model Project (ICFMP). The analysis was conducted with the Consolidated Model for Fire and Smoke Transport (CFAST), a zone model, and Fire Dynamics Simulator (FDS), a computational fluid dynamic model developed by the Building Fire Research Laboratory (BFRL), National Institute of Standards and Technology (NIST). The U.S. Nuclear Regulatory Commission (NRC) is evaluating the CFAST and FDS fire models developed by the National Institute of Standards and Technology for use in NRC's regulatory framework. The objective of the 5th benchmark exercise was to examine cable exposure to pool fires in a trench, and flame spread in vertical cable trays. This validation study shows that most of the sub-models implemented in CFAST and FDS for modeling the physical phenomena in the scenario predicted reasonable trends and magnitudes of global parameters of interest. The predictions of the sub-models for combustion chemistry (tracking concentrations of oxygen and combustion products such as CO2) were reasonable. The plume flows predicted resulted in reasonable accuracy of global compartment parameters, and the mass and energy balance in and out of the compartment. Specifically, the sub-models in the codes for ventilation and heat flow through doors predicted accurate results. Although relatively good performance is noted for most parameters, the calculation of heat flux to and temperature of targets and walls require improvement for both CFAST and FDS. The FDS simulation of plume development and tilting due to varying flow conditions in a compartment require improvement for greater accuracy for fires in complex geometries. Finally, the ability to simulate multi-layer boundaries and targets needs to be implemented in CFAST and FDS for NPP applications.

Table of Contents

Abstract iii

List of Tables vi

List of Figures vii

Executive Summary viii

Foreword x

Acknowledgments xi

1 Introduction 1
- 1.1 Specification of International Benchmarking Exercise # 5 1
  - 1.1.1 Room Geometry 1
  - 1.1.2 Natural Ventilation 3
  - 1.1.3 Mechanical Ventilation 3
  - 1.1.4 Fire 3
  - 1.1.5 Targets 3

2 Input Parameters and Assumptions 4

3 Evaluation of Specified Model Predictions 6
- 3.1 Test 4 6
  - 3.1.1 Global Compartment Parameters 7
  - 3.1.2 Local Gas Temperature 8
  - 3.1.3 Heat Flux to Cable Targets 9
  - 3.1.4 Cable Temperature 10
  - 3.1.5 Wall Temperature 10
  - 3.1.6 Conclusion 11

4 General Recommendations and Conclusions 12
- 4.1 Capabilities 12
- 4.2 Limitations 12
  - 4.2.1 Heat Flux Models in CFAST and FDS 12
  - 4.2.2 Target Models in CFAST and FDS 12
  - 4.2.3 Plume Model in FDS 13
  - 4.2.4 Modeling of Multi-Layer Boundaries with CFAST and FDS 14
- 4.2 User Interface 14
- 4.3 Benefits of Hand Calculations 14
- 4.4 Need for Model Improvements 15
- 4.5 Need for Advanced Models 15
- 4.6 Need for Additional Test Programs 15

References 16

Appendix A Specification of Benchmark Exercise # 5 38

Appendix B Input Data for CFAST and FDS 39

List of Tables

Table 1-1 Wall, Floor, and Ceiling Material 3
Table 1-2 Thermophysical Properties of Wall, Floor, and Ceiling Materials 3
Table 1 Summary of Predictions for Test 4 for CFAST and FDS 17
Table 2 Summary of Predictions with FDTs - Test 4 20

List of Figures

Figure 1-1 Compartment Geometry for Benchmark Exercise # 5 2
Figure 1 Heat Release Rate (CFAST) - Test 4 21
Figure 2 Heat Release Rate (FDS) - Test 4 21
Figure 3 HGL Interface Height - Test 4 22
Figure 4 - Door Flows - Test 4 22
Figure 5 HGL Temperature - Test 4 23
Figure 6 Oxygen Concentration - Test 4 23
Figure 7 CO2 Concentration - Test 4 24
Figure 8 Heat Flow through Door - Test 4 24
Figure 9 Compartment Pressure - Test 4 25
Figure 10 Isosurface of Flame Sheet (40 s) - Test 4 25
Figure 11 Isosurface of Flame Sheet (442 s) - Test 4 26
Figure 12 Temperature Slice View (y=1.8 m, 20 s) - Test 4 26
Figure 13 Temperature Slice View (y=1.8 m, 340 s) - Test 4 27
Figure 14 Temperature Slice View (x=1.8 m, 461 s) - Test 4 27
Figure 15 Flow Vectors in Trench (600 s) - Test 4 28
Figure 16 Isosurface of Flame Sheet (631 s) - Test 4 28
Figure 17 Photograph of Pool Fire in Trench 29
Figure 18 Photograph of Pool Fire in Trench 29
Figure 19 Photograph of Pool Fire in Trench 30
Figure 20 Photograph of Pool Fire in Trench 30
Figure 21 Plume Temperature - Test 4 31
Figure 22 Compartment Temperature (TR1) - Test 4 31
Figure 23 Compartment temperature (TR2) - Test 4 32
Figure 24 Compartment Temperature (TR3) - Test 4 32
Figure 25 Compartment Temperature (TR4) - Test 4 33
Figure 26 Compartment Temperature (TR5) - Test 4 33
Figure 27 Heat Flux on Cables (CFAST) - Test 4 34
Figure 28 Heat Flux on Cables (FDS) - Test 4 34
Figure 29 Power Cable Temperature - Test 4 35
Figure 30 I&C Cable Temperature - Test 4 35
Figure 31 Wall Temperature (TW2-CFAST) - Test 4 36
Figure 32 Wall Temperature - (TW2-FDS) - Test 4 36
Figure 33 Wall Temperature (TW1) - Test 4 37
Figure 34 Outside Wall Temperature - Test 4 37

Executive Summary

The analysis presented in this report was conducted for Benchmark Exercise # 5 in the International Collaborative Fire Model Project (ICFMP). The experiments for the benchmark exercise were conducted at iBMB (Institut für Baustoffe, Massivbau und Brandschutz) of Braunschweig University of Technology, Germany. The analysis was conducted with CFAST, a zone model, and FDS, a computational fluid dynamic model (CFD) developed by the National Institute of Standards and Technology. The U.S. Nuclear Regulatory Commission (NRC) is evaluating the CFAST and FDS fire models developed by the National Institute of Standards and Technology for use in NRC's regulatory framework. The objective of the 5th benchmark exercise was to examine cable exposure to pool fires in a trench, and flame spread in vertical cable trays. The fire scenarios in Benchmark Exercise # 4 are considered to be above average complexity that analysts would model for NPP applications. The scenarios apply to pool fires in complex geometries and flame spread in cable trays.

This validation study shows that most of the sub-models implemented in CFAST and FDS for modeling the physical phenomena in the scenario predicted reasonable trends and magnitudes of global parameters of interest. The predictions of the sub-models for combustion chemistry (tracking concentrations of oxygen and combustion products such as CO2) were reasonable. The plume flows predicted resulted in reasonable accuracy of global compartment parameters, and the mass and energy balance in and out of the compartment. Specifically, the sub-models in the codes for ventilation and heat flow through doors predicted accurate results. Global parameters such as the door mass and heat flows, interface height, and O2 concentration were within 20 % of experimental values. The local gas temperatures in the compartment predicted by FDS were generally within 10 % of experimental observations.

The heat flux to the cables predicted by CFAST and FDS had large inaccuracies and deviated by as much as + 49 % and - 49 % from experimental observation, respectively. There are specific weaknesses in the heat flux models in CFAST and FDS which make them inaccurate for predicting heat fluxes to NPP targets.

A detailed heat transfer model for the cable trays used in the experiments will be fairly complex. The CFAST and FDS fire models are not capable of modeling complex cable tray configurations. The cable targets in these models are represented as rectangular slabs, the slabs were assumed to be of the same thickness as the cables. These limitations of CFAST and FDS for modeling cable targets were noted in ICFMP Benchmark Exercise # 1 [Dey, 2002]. Large uncertainties in the cable temperature predictions by CFAST and FDS were observed in this validation study and are due to the limitations of the heat flux models and the target models. The thermal inertia of the cables reduce the magnitude of the inaccuracies caused by the target models on the cable temperature predictions.

This validation study shows the importance of modeling the plume development in CFD codes to adequately capture all the fire phenomenon in complex geometries, and to evaluate target heat up and ignition near the plume. FDS predicted that the flows that develop in the fire trench in the experiments significantly effects plume development and tilting. Although the main features of the plume development were similar experimental observations, the experiments showed that FDS predictions can be erroneous and lead to large under predictions of plume and target temperatures for pool fires in complex geometries.

The CFAST and FDS codes do not have the capability to model multi-layer boundaries,

The CFAST and FDS codes do not have the capability to model multi-layer boundaries, therefore, a single-layer assumption had to be adopted to model the multi-layer boundaries in the experiments. Although the single-layer assumption did not effect the prediction of the peak values of compartment temperatures, a discrepancy in the gradients of the temperature were noted.

Although relatively good performance is noted above for most parameters, the calculation of heat flux to and temperature of targets and walls require improvement for both CFAST and FDS. The FDS simulation of plume development and tilting due to varying flow conditions in a compartment require improvement for greater accuracy for fires in complex geometries. Finally, the ability to simulate multi-layer boundaries and targets needs to be implemented in CFAST and FDS for NPP applications.

As discussed above, the flame and plume development for a pool fire in a trench can be random, and unpredictable. It will be beneficial to conduct additional tests to examine fire plume development in various geometries for NPP scenarios. These tests will provide data to improve the highly precise plume predictions required of CFD codes for fires in complex geometries.

Acknowledgments

The author wishes to acknowledge the efforts of IBMB and GRS for developing the specification of this exercise for the International Collaborative Fire Model Project. It is recognized that development of such a specification and experimental data requires considerable resources from these organizations. Specifically, the efforts of Olaf Riese and D. Hosser at iBMB, and Marina Rowekamp at GRS, are greatly acknowledged and appreciated. Also, the author thanks the many participants of the International Collaborative Project and this benchmark exercise for their comments on the analysis reported herein, and the useful discussions on the complex fire scenarios analyzed in this exercise.

1 Introduction

The validation study of the CFAST and FDS fire computer codes presented here was conducted as part of Benchmark Exercise # 5 of the International Collaborative Fire Model Project (ICFMP). The USNRC exercised the CFAST and FDS codes, developed by the National Institute of Standards and Technology (NIST), as part of its program to evaluate and validate these computer codes for use in NRC's regulatory framework.

The validation study was conducted using compartment conditions and prescribed heat release rates measured during the experiments. The study was limited to the validation of the codes for predicting compartment conditions and cable target responses to a pool fire in a trench geometry. Therefore, the study only utilized Test 4 which included a pool fire used to preheat the compartment and PVC cables. Test 1 was not simulated since FRNC cables are not utilized in US NPPs. No attempt was made in this study to model cable ignition and flame spread and to use the entire extent of data available from these comprehensive and useful experiments. As part of their research efforts for model development, NIST exercised the FDS code to attempt to predict flame spread in the cable trays observed during the experiments [Riese, 2005]. Although the pyrolysis model within FDS was not designed for this type of simulation, it was nevertheless used to simulate the experiments to the extent the model could, and examine the results to gain some insight into the detailed solid phase behavior. This work is summarized in Section 4.4. The USNRC also sponsored SNL to conduct analysis with their CFD code, VULCAN, to analyze the cable tray flame spread observed in the experiments [Riese, 2005].

The following provides a summary of the specification of the benchmark exercise. A complete specification of the exercise is included in Appendix A.

1.1 Specification of International Benchmarking Exercise # 5

Experiments for cable exposure to pool fires in a trench and flame spread in a compartment were conducted at iBMB (Institut für Baustoffe, Massivbau und Brandschutz) of Braunschweig University of Technology, Germany and used for this benchmark exercise.

1.1.1 Room Geometry

The experimental room (see Figure 1.1) has a floor area of 3.6 m x 3.6 m and a height of 5.6 m. The room is made of concrete and is naturally ventilated. The surface materials as well and the thermophysical properties of those materials are listed in Tables 1-1 and 1-2.

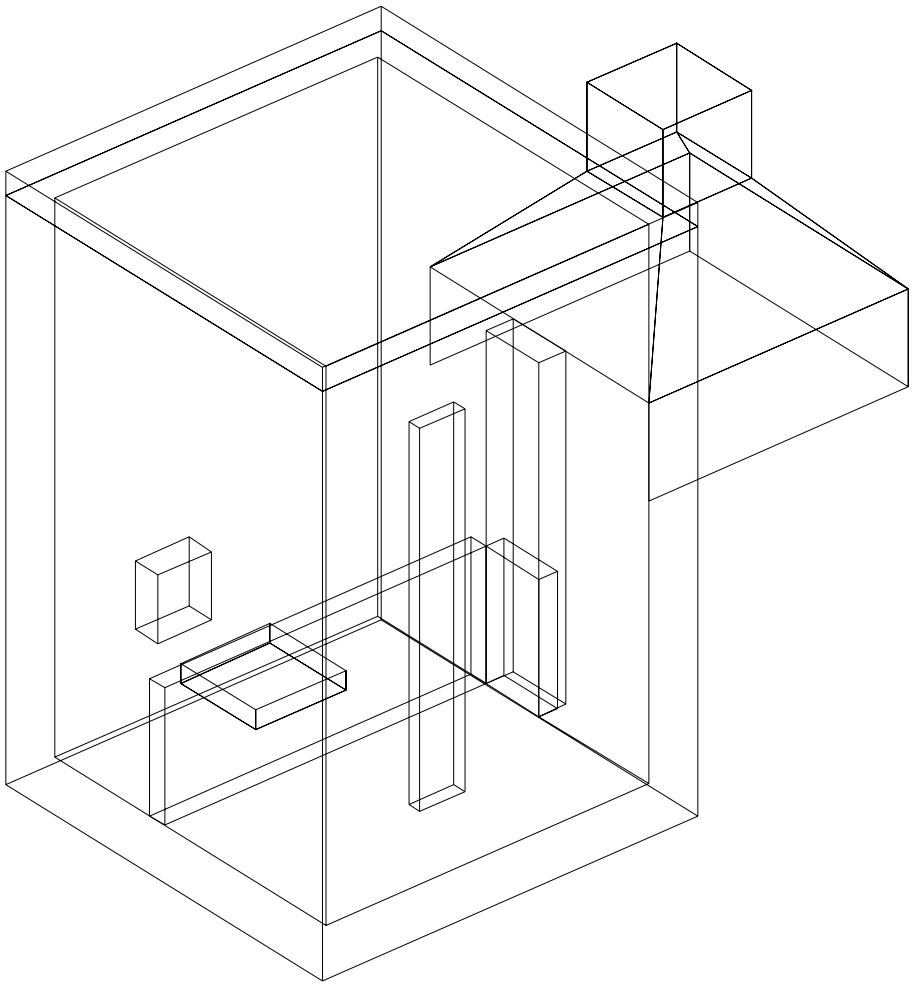

Figure 1-1 Compartment Geometry for Benchmark Exercise # 5

Table 1-1 Wall, Floor, and Ceiling Material

Surface	Material	Thickness [m]
Floor	Concrete	0.30
Side walls	Light concrete	0.25
	Insulation	0.05
Ceiling	Light Concrete	0.20
Walls, 1.4 m ht.	Aerated Concrete	0.20

Table 1-2 Thermophysical Properties of Wall, Floor, and Ceiling Materials

Material	Thermal conductivity [W/m K]	Specific Heat [kJ/kg K]	Density [kJ/m^3]
Concrete	2.10	880	2400
Aerated concrete	0.75	840	1500
Light concrete	0.11	1350	420
Insulation	0.05	1500	100

1.1.2 Natural Ventilation

The gas exchange takes place through an opening of 0.7 m width and 3.6 m height, which is reduced by a wall of 1.4 m height to an area of approx. 1.5 m².

1.1.3 Mechanical Ventilation

The selected test compartment was not mechanically ventilated.

1.1.4 Fire

The first part of the selected test consisted of preheating the cable trays in the room. A pool 1 m² floor area filled with ethanol (ethylene alcohol) located in a trench is used as the pre-heating source. This 1st part of the experiment was used for this validation study.

A hood was installed above the front door (See Figure 1-1). Using the oxygen consumption method the energy release can be estimated.

1.1.5 Targets

Two vertical cable trays were located along the height of the compartment on the opposite side of the pool fire which was enclosed by a 1.4 m wall. The two cable trays were filled with power cables and I&C cables, respectively. For the Test 4 which is used in this validation study, the cables were composed of PVC material.

2 Input Parameters and Assumptions

A comprehensive specification of Benchmark Exercise # 5 was developed such that there would be a minimal amount of unspecified parameters and assumptions for the analysts conducting specified[1] predictions for the exercise. However, there were still some parameters for which values had to assumed for conducting the specified calculations. These are listed and discussed below:

1. Heat Release Rate (HRR): The HRRs of the fire measured during the experiments are used for this validation study. The measured HRR deviated from the HRR planned and stated in the specification of the exercise by ~ 20 %. Therefore, the calculations made for the specified HRR were redone with the measured values after the release of experimental data.

2. Oxygen Content in Fuel: Ethanol (CH_3CH_2OH) is the 1st fuel used in the ICFMP benchmark exercises that contained oxygen. Problems were faced in specifying the O2/C ratio input for CFAST. Specifying the O2/C ratio based on directions in the CFAST User's Guide resulted in an inadvertent increase of the specified HRR. An inconsistency existed between the source code and directions in the User's Guide which had to be resolved for correct implementation of the input data.

3. Target Specification: A detailed heat transfer model for a cable or cable tray will be fairly complex. Cable trays generally have a number of cables bundled together in layers, and most cables consist of several conductors. Cables configured in a single layer will get damaged and ignite at a lower flux than cables in a multilayer configuration because the flux to a single layer will not be shielded by cables above that layer. The damage or ignition temperature for cables in a multilayer configuration will depend on the volume-to-surface area ratio. The CFAST and FDS fire models are not capable of modeling complex cable configurations. The target in these models is represented as rectangular slabs, the slabs were assumed to be of the same thickness as the cables. Similar limitations of CFAST and FDS for modeling cable targets were noted in ICFMP Benchmark Exercise # 1 [Dey, 2002].

4. Material Properties of Walls and Targets: The material properties of the walls, ceiling, floor, and targets were specified for the exercise using values available in the literature for these materials. The properties of the specific materials used in the experiments may vary from the generic values reported in the literature. This may a source of uncertainty in the predicted results.

5. Radiative Fraction: The radiative fraction of the fuel was specified based on values in the FDS database for ethanol. The radiative fraction for ethanol in the specific configuration for the benchmark exercise may vary from the value in the FDS database. The value of 0.2 for the radiative fraction in the FDS database seemed low, therefore, the value of 0.25 from a fire protection handbook [SFPE, 1995] was used for the calculations. This assumption may have an impact on the predicted results since this parameter determines the convective and radiative heat flow from the plume in both CFAST and

[1] As defined in ASTM 1355 [ASTM, 2005].

FDS fire codes. This parameter was identified as a key parameter effecting fire compartment conditions in ICFMP Benchmark Exercise # 2 [Miles, 2004].

6. Grid Size: A grid size of 10 cm was used for the FDS calculations. It is recognized that CFD calculations are generally sensitive to the grid used. A grid size of 10 cm may be optimal for the type of scenarios simulated, however, this was not confirmed through a grid sensitivity analysis.

7. Multi-Layer Boundaries: The layer of insulation covering the walls was neglected in the CFAST calculation since it could not be directly modeled in CFAST. An insulated or adiabatic boundary condition was imposed on the walls for the FDS calculations.

8. Exhaust Hood: FDS calculations were conducted with and without the exhaust hood above the door of the compartment to determine its effect on the compartment conditions. It was determined that modeling the hood had very little effect on the compartment conditions. Therefore, no attempt was made to account for the exhaust hood as part of a ventilation system in the CFAST calculations.

9. Heat Flux Comparisons: The comparison of heat flux prediction with measured data poses several challenges. It is important that equivalent measures of heat flux are used in the comparison. The flux gauges in the experiments in benchmark Exercise # 5 were cooled and maintained at a constant temperature (20 C). The CFAST and FDS codes normally output the net heat flux on targets based on the target temperature. It is important that these fluxes be modified to the incident radiative heat flux and the convective heat flux to a block at constant temperature for comparison with measured heat fluxes. Even with the modifications to account for the differences between measured and predicted values, an exact comparison is not possible due to the lack of ability to exactly measure the calculated values from models. Therefore, the comparison of heat fluxes will have some additional uncertainty due to this limitation.

3 Evaluation of Specified Model Predictions

The following provides a comparison of predictions by CFAST and FDS with results of Test 4 conducted for ICFMP Benchmark Exercise # 5. The results of CFAST, a zone model, and FDS, a CFD code, are presented together to allow a comparison and discussion of the capabilities and limitations of the two types of models. Predictions using CFAST and FDS were made using the specified HRR and sent to GRS before the experimental data was released by them. GRS has certified the authenticity of these specified[2] calculations. However, as indicated above, the measured HRR deviated from that provided for the specified exercise. Therefore, the specified calculations were redone after the release of experimental data using exactly the same input data except for the measured HRR. These predictions are compared with the experimental data and presented below. The input data files for CFAST and FDS are included in Appendix B.

The following is a list of the major sub-models implemented in the two fire computer codes for modeling the physical phenomena in the scenarios:

- combustion chemistry (tracking concentrations of oxygen and combustion products)
- plume and ceiling jet flow
- mass and energy balance
- ventilation through doors
- forced ventilation
- heat transfer to boundaries
- heat transfer to targets
- thermal response of the target

The FDS code computes the flows from first principles based on fluid dynamic equations, whereas CFAST utilizes correlations developed from experimental data. The performance of these sub-models is discussed below based on comparison of predicted results with experimental measurements. The theoretical formulation of the two models may be found in Jones, 2004 for CFAST, and McGrattan, 2004 for FDS. The theoretical formulation of these codes are presented in these reports according to the format and content required by ASTM - 1355, “Evaluating the Predictive Capability of Deterministic Fire Models,” [ASTM, 2005]. These reports were sponsored by the U.S. Nuclear Regulatory Commission for referencing in its validation studies as that reported herein.

3.1 Test 4

The following presents the comparison of predictions by the CFAST and FDS code with experimental data for Test 4 of the series. The discussion is grouped in categories presented below to evaluate the predictive capability of the models according to the general features and sub-models of the codes:

- Global parameters
- Local gas temperature
- Heat flux to targets

[2] As defined in ASTM-1355 [ASTM, 2005].

- Target temperature
- Wall temperature

Figures 1 to 34 show the comparison of the trends of the predictions of CFAST and FDS with experimental data, and Table 1 shows the peak values predicted by the models and that measured, and the uncertainty of the predictions. The uncertainty value tabulated is:

(model prediction at peak- measured value at peak)/(measured value at peak - initial measured value)

A + sign in the uncertainty value means that the model prediction was greater than the measured value, and a - sign means that the model prediction was less than measured value

3.1.1 Global Compartment Parameters

The HRR measured during the test and prescribed as input to the CFAST and FDS models are shown in Figures 1 and 2. The HRR increases rapidly to 250 kW in ~ 265 s, and then increases more gradually to ~ 350 kW. Both CFAST and FDS follow the prescribed HRRs based on experimental data. There is no decrease in the HRR after 1200 s because the second phase of this experiment for pilot ignition of the cables was initiated at this point. As indicated above, this second phase of the experiment was not modeled for this validation study.

Figure 3 shows the development of the hot gas layer. The CFAST and FDS predictions, and experimental measurement all show that the HGL interface height reaches a steady level of ~ 1.5 m (just above bottom of door) in ~ 60 s. Table 1 shows the steady state HGL interface height predicted by the codes and measured, and the uncertainties in the CFAST and FDS predictions. CFAST and FDS over-predict the steady state HGL interface height by + 6 % and + 11 %, respectively.

Figure 4 compares the door mass flows predicted by the codes and measured. An error exists in the measured flow into the compartment since it should be equal to the flow out of the compartment. FDS prediction of flow in and out of the compartment at ~ 1 kg/s is the same as measurement. CFAST over predicts the flows at ~ 1.2 kg/s by + 20 %.

Figure 5 shows the hot gas layer (HGL) temperature. Both CFAST and FDS predictions are similar to experimental observation, rapidly reaching ~ 140 C in ~ 60 s followed by a more gradual increase to 180 C at the end of the transient.

Figure 6 compares the O2 depletion predicted by CFAST and FDS with experiment. The trend is similar to the HRR which determines the O2 consumption. The O2 level at GA2, located at 4.4 m above the floor in the HGL, predicted by CFAST and FDS at the end of the transient is 18.4 % and 18.0 %, respectively. The measured O2 level at the end of the transient is 18.9 %. Since the decrease in O2 level is very small and close to measurement uncertainties, the uncertainties in the predicted quantities are not reported.

Figure 7 compares the CO2 production predicted by CFAST and FDS with experiment. The trend is similar to the HRR which determines the CO2 production. The CO2 level at GA2, located at 4.4 m above the floor in the HGL, predicted by CFAST and FDS at the end of the transient is 0.8 % and 1.6 %, respectively. The measured CO2 level at the end of the transient is 1.3 %. The uncertainties in the CFAST and FDS predictions are - 37 % and + 20 %,

respectively.

Figure 8 compares the door heat flows predicted by FDS and measurement. The FDS prediction of heat flow out of the compartment at ~ 166 kW is the same as measured. The CFAST code does not output this parameter.

Figure 9 compares the pressure predicted by CFAST and FDS in the compartment with measurement. The pressures predicted and measured at or near the floor are very similar and small, in the order of 2-3 Pa. The negative pressure indicates that flow will be into the compartment, as discussed later. Since the pressures are small and within the measurement uncertainties, the uncertainties of the predicted quantities are not reported.

3.1.2 Local Gas Temperature

The local gas temperatures in the plume, ceiling jet, and compartment are only predicted by FDS. FDS outputs showing plume and HGL development is shown in Figures 10-14. Figure 10 shows an isosurface of the mixture fraction (at a value of 0.099), which represents the flame sheet created by FDS at ~ 40 s. The figure shows that the plume is mainly vertical at this time. Figure 11 shows an isosurface of the mixture fraction (at a value of 0.099) at 442 s. The figure shows that the plume takes a different form and is drawn to the right wall at this point. A review of the isosurface of the mixture fraction through the transient with Smokeview indicates that the plume is vertical until ~ 90 s and then oscillates with random shapes between the right wall and the partial wall (1.4 m height) on the left. The fire plume seems to effected by the trench geometry between the two walls. Figures 12 and 13 show a temperature slice at y = 1.8 m at 20 s and 340 s, again indicating a vertical plume at the beginning of the transient followed by a plume which takes random shapes and is confined by the surrounding walls. Figure 14 shows a temperature slice at x = 1.8 m which illustrates the flow of ambient air into the compartment through the door. The figure also shows the HGL above the bottom of the door, and illustrates the temperature gradient in the HGL. Figure 15 shows the flow vectors in the fire trench between the partial and right walls. The figure shows that the flow into the compartment from the door causes a reverse flow in the trench pushing the fire plume toward the front wall. Figure 16 shows an isosurface of the flame sheet and confirms the tilting of the fire plume toward the front wall. This reverse flow of air into the fire plume results in its tilting and possibly also the random shapes. Sufficient measurements were not available to confirm all the features of the FDS plume predictions. However, Figures 17-20 which show photographs of the fire within a 1-minute time frame confirm the general random nature of the flame in the trench.

Figure 21 shows the comparison of measured plume temperatures at TP2 - TP7 with that predicted by FDS. As shown in Figure 21, FDS predicts peaks in the plume temperature at ~ 120 s. These peaks are explained by the plume development predicted by FDS. As discussed above, observations of the plume predicted by FDS through Smokeview (the graphical interface for FDS) indicates a steady vertical plume until ~ 90 s when the plume begins to oscillate with random shapes between the left partial wall and right wall. This results in the FDS predictions of peaks in the plume temperature, specifically at the lower level at TP2 and TP3. The experimental measurements at TP2 and TP3 show an oscillation in the temperature which indicates movement of the plume. Measurements indicate that TP4 - TP7 are sensing the HGL temperature and that the plume does not extend to the higher levels. The plume temperature measurement by itself cannot confirm the plume is behaving in the manner predicted by FDS. The measured data shows the plume to be fully developed at ~ 60 s after which the plume temperatures at TP2 increases to ~ 450 C without any intermediate peaks. FDS predicts the

plume temperatures to reach ~ 180 C at the end of the transients indicating the temperature in the plume region at this time is the same as in the HGL. This again confirms the behavior of the plume predicted by FDS which results in the centerline of the plume above the fire to be at the temperature of the HGL. As shown in Table 1, the uncertainty in the predicted values are - 46 %, - 10 %, and + 1 % for TP3, TP5, and TP7, respectively.

Figure 22 shows the local gas temperatures in the compartment at TR1. TR 1-3 is near the HGL interface and reads a lower temperature than TR 1-5 and TR 1-7. FDS predicts a higher temperature than measured at TR 1-3 and TR 1-5, and similar temperatures for TR 1-7. FDS predicts a very small temperature gradient between TR 1-5 and TR 1-7, whereas measurements indicate a steeper temperature gradient.

Figure 23 shows the local gas temperature in the compartment at TR 2. FDS predictions are similar to measurements at this location. Figure 24 shows the local gas temperatures at TR 3 which is located near the back wall. The predicted values are similar to measurements. Oscillations in the temperature predictions by FDS at this point are noted, especially at the lower levels for TR 3-3 and TR 3-5. These oscillations are possibly caused by the reversed flow in the trench as discussed above. Figure 25 shows the local gas temperatures at TR 4 which is also located near the back wall. Oscillations in the gas temperature at this point are also noted, especially at the lower level at TR 4-3. Finally, Figure 26 shows the local gas temperatures at TR 5 near the cables. Again, FDS predictions are similar to measurements with uncertainties of + 8 %, + 4 %, and + 5 % at TR 5-3, TR 5-5, and TR 5-7, respectively.

3.1.3 Heat Flux to Cable Targets

Figures 27 shows a comparison of the total heat flux on the cables predicted by CFAST and experiment. The heat flux on the gauges WS2 and WS3 on the left wall are mainly due to the flux from the HGL since the 1.4 m wall shields the gauges from most of the radiative heat flux from the fire. The experimental measurement of heat flux at WS 1 is very small since it is not in the HGL, and the 1.4-m partial wall shields the radiative heat flux from the fire. The CFAST prediction at WS1 is not included since CFAST does not have the capability to include partial walls in the compartment geometry. The measured fluxes at WS2, WS3, and WS4 is increasingly higher due to the temperature gradient in the HGL. The heat fluxes predicted by CFAST for WS2, WS3, and WS4 are of similar magnitude since only the average HGL temperature is predicted in a zone model, and temperature gradients in the hot gas are not simulated in such a model. The large oscillations in the measured heat flux, especially at WS3 and WS4, may be due to the position of the flux gauges in between the vertical cable trays and disturbance of the flow field by the cable trays in those positions.

Figure 28 shows a comparison of the total heat flux on the cables predicted by FDS and experiment. Although the FDS prediction at WS2 is lower than at the other gauges, the predicted heat flux levels at WS3, WS4, and WS5 are similar in magnitude. FDS does not predict the variation and gradient in the heat flux versus elevation, as measured. The uncertainties of the peak predicted heat fluxes for WS2, WS3, and WS4 for CFAST are + 49 %, 0 %, and - 15 %, respectively; and for FDS are - 49 %, - 42 %, and - 45 %, respectively.

3.1.4 Cable Temperature

Figure 29 shows a comparison of the surface temperature of the power cable predicted by CFAST and FDS with experiment. The measured cable surface temperature at different

elevations shows gradient similar to that observed for the heat flux. However, the measured temperature at TCO 1-5 is greater than at TCO 1-7, contrary to expectation that temperatures in the HGL increase with elevation. The predictions by CFAST at the different elevations are similar in magnitude, as discussed above. The predictions by FDS show variations in the temperature at TCO 1-1 and TCO 1-3, but the temperatures at the other elevations are of similar magnitude. The uncertainties of the peak predicted surface temperatures for the power cable at TCO 1-3, TCO 1-5, and TCO 1-7 for CFAST are + 2 % %, - 23 %, and - 21 %, respectively; and for FDS are - 41 %, - 32 %, and - 26 %, respectively.

Figure 30 shows a comparison of the surface temperature of the I&C cable predicted by CFAST and FDS with experiment. The measured cable surface temperature at different elevations shows a gradient similar to that observed for the heat flux. However, the measured temperature at TCO 3-5 is greater than at TCO 3-7, contrary to expectation. The predictions by CFAST at the different elevations are similar in magnitude, as discussed above. The predictions by FDS show variations in the temperature at TCO 3-1 and TCO 3-3, but the temperatures at the other elevations are of similar magnitude. The uncertainties of the peak predicted surface temperatures for the I&C cable at TCO 3-3, TCO 3-5, and TCO 3-7 for CFAST are - 16 %, - 35 %, and - 33 %, respectively; and for FDS are - 55 %, - 48 %, and - 44 %, respectively.

3.1.5 Wall Temperature

Figure 31 shows a comparison of left wall temperatures at TW-2 predicted by CFAST with experiment. The measured wall surface temperature at different elevations shows a gradient similar to that observed for the heat flux. However, the measured temperature at TW 2-4 is greater than at TW 2-5, contrary to expectation. Although the predicted and measured values are similar in magnitude at TW 2-4 and TW 2-5, the prediction at TW 2-2 is much larger than measurement. This is due to the lack of capability in CFAST to model the partial 1.4-m wall. CFAST is predicting a higher than actual radiative flux from the fire at TW 2-2 due to this limitation. The uncertainties of the peak wall surface temperatures at TW 2-2, TW 2-4, and TW 2-5 are + 250 % (see reason above), - 12 %, and 0 %, respectively.

Figure 32 shows a comparison of left wall temperatures at TW-2 predicted by FDS with experiment. The FDS predictions are similar in magnitude to measured values. The uncertainties of the peak wall surface temperatures at TW 2-2, TW 2-4, and TW 2-5 are - 42 %, - 30 %, and 11 %, respectively.

Figure 33 shows a comparison of the rear wall temperatures at TW-1 predicted by FDS with experiment. FDS predictions are ~ 20 % less than measured values.

Finally, Figure 34 shows FDS predictions of the back wall temperature compared with experimental observations. Since an adiabatic assumption (see above) was adopted for the walls in FDS to compensate for the lack of ability to model multi-layer boundaries, the temperature predicted at the back wall is constant. The measured back wall temperatures at TW 2 and TW 1 essentially remain at a constant temperature, decreasing slightly only due to temperature fluctuations in the compartment. This confirms the validity of the adiabatic assumption adopted in the FDS calculation.

3.1.6 Conclusion

CFAST and FDS predictions were similar to experimental observations for most parameters.

Global parameters such as the door mass and heat flows, interface height, and O2 concentration were within 20 % of experimental values. Except for TP3, the local gas temperatures in the compartment and in the plume predicted by FDS were generally within 10 % of experimental observations. The effect of flows in the trench impacted the characteristics of plume development and temperature predicted by FDS. The heat flux to the cables predicted by CFAST and FDS deviated by as much as + 49 % and - 49 % from experimental observation, respectively. The corresponding cable surface temperatures predicted by CFAST and FDS deviated by as much as 35 % and 55 % from experimental observation, respectively.

4 General Recommendations and Conclusions

The following provides the findings and conclusions of this validation study. The fire scenarios in Benchmark Exercise # 5 are considered to be of above average complexity that analysts would model for NPP applications. The scenarios apply to indirect vertical cable tray exposure to pool fires.

4.1 Capabilities

This validation study shows that most of the sub-models implemented in both fire computer codes for modeling the physical phenomena in the scenario predicted reasonable trends and magnitudes of global parameters of interest. The predictions of the sub-models for combustion chemistry (tracking concentrations of oxygen and combustion products such as CO2) were reasonable. The plume flows predicted resulted in reasonable accuracy of global compartment parameters, and the mass and energy balance in and out of the compartment. Specifically, the sub-models in the codes for ventilation and heat flow through doors predicted accurate results. Global parameters such as the door mass and heat flows, interface height, and O2 concentration were within 20 % of experimental values. The local gas temperatures in the compartment predicted by FDS were generally within 10 % of experimental observations.

4.2 Limitations

4.2.1 Heat Flux Models in CFAST and FDS

The heat flux to the cables predicted by CFAST and FDS had large inaccuracies and deviated by as much as + 49 % and - 49 % from experimental observation, respectively.

Figures 27 showed a comparison of the total heat flux on the cables predicted by CFAST and experiment. The measured fluxes at WS2, WS3, and WS4 is increasingly higher due to the temperature gradient in the HGL. The heat fluxes predicted by CFAST for WS2, WS3, and WS4 are of similar magnitude since only the average HGL temperature is predicted in a zone model, and temperature gradients in the hot gas are not simulated in such a model. Figure 28 shows a comparison of the total heat flux on the cables predicted by FDS and experiment. FDS does not predict the variation and gradient in the heat flux versus elevation, as measured. The uncertainties of the peak predicted heat fluxes for WS2, WS3, and WS4 for CFAST are + 49 %, 0 %, and - 15 %, respectively; and for FDS are - 49 %, - 42 %, and - 45 %, respectively.

Figure 31 showed a comparison of left wall temperatures at TW-2 predicted by CFAST with experiment. The measured wall surface temperature at different elevations shows a gradient similar to that observed for the heat flux. The prediction at TW 2-2 is much larger than measurement by 250 %. This is due to the lack of capability in CFAST to model the partial 1.4-m wall. CFAST is predicting a higher than actual radiative flux from the fire at TW 2-2 due to this limitation.

There are specific weaknesses in the heat flux models in CFAST and FDS which make them inaccurate for predicting heat fluxes to NPP targets.

4.2.2 Target Models in CFAST and FDS

A detailed heat transfer model for the cable trays used in the experiments will be fairly complex. The CFAST and FDS fire models are not capable of modeling complex cable tray configurations. The cable targets in these models are represented as rectangular slabs, the slabs were assumed to be of the same thickness as the cables. These limitations of CFAST and FDS for modeling cable targets were noted in ICFMP Benchmark Exercise # 1 [Dey, 2002]. Figure 29 showes a comparison of the surface temperature of the power cable predicted by CFAST and FDS with experiment. The measured cable surface temperature at different elevations shows gradient similar to that observed for the heat flux. The predictions by CFAST at the different elevations are similar in magnitude, as discussed above. The uncertainties of the peak predicted surface temperatures for the power cable at TCO 1-3, TCO 1-5, and TCO 1-7 for CFAST are + 2 % %, - 23 %, and - 21 %, respectively; and for FDS are - 41 %, - 32 %, and - 26 %, respectively. Figure 30 showed a comparison of the surface temperature of the I&C cable predicted by CFAST and FDS with experiment. The uncertainties of the peak predicted surface temperatures for the I&C cable at TCO 3-3, TCO 3-5, and TCO 3-7 for CFAST are - 16 %, - 35 %, and - 33 %, respectively; and for FDS are - 55 %, - 48 %, and - 44 %, respectively.

The large uncertainties in the cable temperature predictions by CFAST and FDS are due to the limitations of the heat flux models and the target models. The thermal inertia of the cables reduce magnitude of the inaccuracies caused by the target models on the cable temperature predictions.

4.2.3 Plume Model in FDS

The study shows the importance of accurately modeling the plume development in CFD codes to adequately capture all the fire phenomenon, and to evaluate target heat up and ignition near the plume. FDS predicted that the flows that develop in the fire trench significantly effects plume development and tilting.

FDS outputs showing plume and HGL development is shown in Figures 10-14. Figure 10 shows the flame sheet created by FDS at ~ 40 s. The figure shows that the plume is mainly vertical at this time. Figure 11 shows the flame sheet at 442 s. The figure shows that the plume takes a different form and is drawn to the right wall at this point. A review of the flame sheet through the transient with Smokeview indicates that the plume is vertical until ~ 90 s and then oscillates with random shapes between the right wall and the partial wall (1.4 m height) on the left. The fire plume seems to be effected by the trench geometry between the two walls. FDS predicts a reverse flow of air in the trench into the fire plume which results in its tilting and possibly also the random shapes. Sufficient measurements were not available to confirm all the features of the FDS plume predictions. However, Figures 17-20 which show photographs of the fire within a 1-minute time frame confirm the general random nature of the flame in the trench.

Figure 21 shows the comparison of measured plume temperatures at TP2 - TP7 with that predicted by FDS. As shown in Figure 21, FDS predicts peaks in the plume temperature at ~ 120 s. These peaks are explained by the plume development predicted by FDS, specifically at the lower level at TP2 and TP3. The measured data shows the plume to be fully developed at ~ 60 s after which the plume temperatures at TP2 increases to ~ 450 C without any intermediate peaks. FDS predicts the plume temperatures to reach ~ 180 C at the end of the transients indicating the temperature in the plume region at this time is the same as in the HGL. This again confirms the behavior of the plume predicted by FDS which results in the centerline of the plume above the fire to be at the temperature of the HGL which is contrary to experimental observation. The uncertainty in the predicted value at TP3 is - 46 %.

The above observations show that FDS predictions can be erroneous and lead to large under predictions of plume and target temperatures for pool fires in complex geometries.

4.2.4 Modeling of Multi-Layer Boundaries with CFAST and FDS

The CFAST and FDS codes do not have the capability to model multi-layer boundaries, therefore, a single-layer assumption had to be adopted to model the aerated concrete around the fuel pan and the concrete floor below. The layer of insulation covering the walls and ceiling was neglected in the calculations since it could not be directly modeled in CFAST or FDS. Although the single-layer assumption did not effect the prediction of the peak values of compartment temperatures, a discrepancy in the gradients are noted in Figure 5 and Figures 26-30.

4.2 User Interface

FDS

The FDS manuals (Technical Reference Guide and User's Guide), in conjunction with the Smokeview graphical interface for reviewing results of the computations, provide a useful interface for the user. The quality of this interface has positively impacted the capability to analyze and interpret the predicted results.

CFAST

Although the Technical Reference Guide for CFAST is detailed, its relationship to the User's Guide, and a useful and comprehensive User's Guide is lacking. Additionally, the graphical user interface (GUI) for CFAST is outdated and does not function in more recent operating platforms such as Windows XP. It would be beneficial to have a comprehensive User's Guide and enhanced GUI to allow more accurate input of data for the simulations and understanding of output parameters such as their units.

The users of these codes should be knowledgeable of the complexities of the compartment conditions, such as plume development in specific geometries, to assess and utilize the results of their calculations.

4.3 Benefits of Hand Calculations

In order to evaluate the benefits of hand calculations, specified calculations with FDTs [NRC, 2004] were conducted. The comparisons show that hand calculations could provide a method to quickly calculate global parameters (such as interface height), as well as plume temperatures using simple correlations. Some large deviations for plume temperature are noted. The plume correlation is for fires in an open environment and does not include the complex effects of the surrounding walls. Since the ranges of validity of the correlations are narrow, the results are best suited for a screening calculation where a rough estimate is required, while acknowledging the answers may contain inaccuracies.

4.4 Need for Model Improvements

Although relatively good performance is noted above for most parameters, the calculation of

heat flux to targets and walls require improvement for both CFAST and FDS. The target models also require improvement to analyze NPP targets. The FDS simulation of plume development and tilting due to varying flow conditions in a compartment require improvement. Finally, the ability simulate multi-layer boundaries and targets needs to be implemented in CFAST and FDS for NPP applications.

As indicated in Chapter 1, FDS was used to simulate cable ignition and flame spread [Riese, 2005]. The bundled cables were modeled as thin-skinned solids. In some of the tests, the cable surface temperature predictions followed the measurements to some extent, but could not simulate the behavior beyond ignition. The qualitative trends in the measured cable temperature were not captured by the model. Clearly, FDS in its current form is not suited for this type of prediction. Engineers using FDS to study actual fires have often "tuned" the solid phase parameters to match a given experiment, but this should be considered *calibration,* not *validation.* Since FDS lacks the ability to resolve the cables and the air gap between them, a purely deterministic model would be impractical. A combination of two general approaches may be possible, empirical and deterministic. An empirical model would use data from experiments to determine burning and flame spread rates, and would avoid directly computing the complex chemical and heat transfer phenomena in the cable trays. Such a model could be coupled with the gas thermal environment predicted by FDS.

4.5 Need for Advanced Models

Simple hand calculations and zone models may be generally suitable for scenarios as in this validation study. However, this study has showed that, the evaluation of target heat up and ignition near the plume region will require the use of accurate and validated CFD codes.

The computational requirements for CFD codes should be noted. The test in this benchmark exercise required 10 hours to compute with FDS, whereas, zone models can be executed in less than 10 s.

4.6 Need for Additional Test Programs

As discussed above, the flame and plume development for a pool fire in a trench can be random, and unpredictable. It will be beneficial to conduct additional tests to examine fire plume development in various geometries for NPP scenarios. These tests will provide data to improve the highly precise plume predictions required of CFD codes for fires in complex geometries.

References

American Society of Testing and Materials, “Evaluating the Predictive Capability of Deterministic Fire Models,” ASTM E1355-04, West Conshohocken, PA (2005).

Dey, M ., Ed., “Evaluation of Fire Models for Nuclear Power Plant Applications,” U.S. Nuclear Regulatory Commission, NUREG-1758, Washington DC, USA, June 2002.

Jones, W., Ed., “CFAST - Consolidated Model of Fire Growth and Smoke Transport (Version 5), National Institute of Standards and Technology, NIST Special Publication 1030, October 2004.

McGrattan, K., Ed., “Fire Dynamics Simulator (Version 4), Technical Reference Guide,” National Institute of Standards and Technology, NIST Special Publication 1018, September 2004.

Miles, S., Ed., “Evaluation of Fire Models for Nuclear Power Plant Applications: Pool Fires In Large Halls,” Building Research Establishment, BRE Report No. 212214, May 2004, Watford, UK.

Riese, O., Ed., “Evaluation of Fire Models for Nuclear Power Plant Applications: Flame Spread in Cable Tray Fires,” to be published.

Society of Fire Protection Engineers, “The SFPE Handbook of Fire Protection Engineering,” 2nd Edition, Bethesda, Maryland, 1995.

U.S. Nuclear Regulatory Commission, " Fire Dynamics Tools (FDTs) Quantitative Fire Hazard Analysis Methods for the U.S. Nuclear Regulatory Commission Fire Protection Inspection Program," NUREG-1805, Washington DC, USA, November 2004.

Table 1 Summary of Predictions for Test 4 for CFAST and FDS

Parameter	Sensor	Model Prediction at Peak		Measured Value at peak	Initial Measured Value	Uncertainty	
		CFAST	FDS			CFAST	FDS
Global Parameters							
HGL Interface Ht		1.6 m	1.8 m	1.3 m	5.7 m	+ 6 %	+ 11 %
HGL Temp. (average)		187 C	176 C	170	19 C	+ 10 %	+ 3.5 %
Door Mass Flow		1.2 kg/s	1 kg/s	1 kg/s	0	+ 20 %	0 %
Door Heat Flow		NA	166 kW	166 kW	0	NA	0 %
Smoke Conc.	NA						
Pressure	DP 5-1	- 1.7 Pa	- 3.2 Pa	- 2.4 Pa	0	NA	NA
Flame Height	NA						
O2 Conc.	GA 2	18.4 %	18.0 %	18.9 %	20.6 %	NA	NA
CO2 Conc.	GA2	0.84 %	1.6 %	1.33 %	0 %	- 37 %	+ 20 %
CO Conc.	GA2					NA	NA
Local Gas Temperature							
Plume Temp.	TP 3		159 C	272 C	19 C		- 46 %
	TP 5		183 C	202 C	19 C		- 10 %
	TP 7		192 C	190 C	19 C		+ 1 %
Hot Gas Temp. (point values)	TR 5-3		122 C	114 C	19 C		+ 8 %

	TR 5-5		192 C	185 C	19 C		+ 4 %
Ceiling Jet Temp.	TR 5-7		193 C	184 C	19 C		+ 5 %
	TR 2-7		185 C	185 C	19 C		0 %
	TR 1-7		195 C	195 C	19 C		0 %
Heat Flux to Cables							
Radiative Heat Flux to Cables	NA						
Total Heat Flux to Cables	WS 2	4 kW/m2	1.4 kW/m2	2.7 kW/m2	0	+ 49 %	- 49 %
	WS 3	3.7 kW/m2	2.1 kW/m2	3.7 kW/m2	0	0 %	- 42 %
	WS 4	3.6 kW/m2	2.3 kW/m2	4.3 kW/m2	0	- 15 %	- 45 %
Cable Temperature							
Cable Surface Temp.	TCO 1-3 (power cable)	106 C	69 C	104 C	19 C	+ 2 %	- 41 %
	TCO 1-5	103 C	93 C	128 C	19 C	- 23 %	- 32 %
	TCO 1-7	104 C	98 C	126 C	19 C	-21 %	- 26 %
	TCO 3-3 (control cable)	112 C	69 C	130 C	19 C	- 16 %	- 55 %
	TCO 3-3	113 C	94 C	164 C	19 C	- 35 %	- 48 %
	TCO 3-7	113 C	98 C	159 C	19 C	- 33 %	- 44 %
Total Heat Flux to Plates/Blocks	NA						

Plates/ Blocks Surface Temp.	NA						
Heat Flux to Walls	NA						
Wall Temperature							
Wall Surface Temp	TW 2-2	65 C	26 C	32 C	19 C	+ 250 %	- 42 %
	TW 2-4	79 C	66 C	87 C	19 C	-12 %	- 30 %
	TW 2-5	77 C	71 C	77 C	19 C	0 %	- 11 %

Notes:
+ Model prediction was greater than measured value
- Model prediction was less than measured value
Value tabulated is: (model prediction at peak- measured value at peak)/(measured value at peak - initial measured value)

Table 2 Summary of Predictions with FDTs - Test 4

Parameter	Sensor	Model prediction at peak	Measured value at peak	Initial measured value	Uncertainty
Global Parameters					
HGL Interface Ht		0.3 m @ 60 s	1.3 m	5.7 m	- 18 %
HGL Temp. (Average)		178 C @ 1200 s	NA	19 C	NA
Local Gas Temperature					
Plume Temp.	TP 3	410	272 C	19 C	+ 62 %
	TP 5	142	202 C	19 C	- 22 %
	TP 7	84	190 C	19 C	- 50 %
Target Heat Flux	NA				

Notes:
+ Model prediction was greater than measured value
- Model prediction was less than measured value
Value tabulated is: (model prediction at peak- measured value at peak)/(measured value at peak - initial measured value)

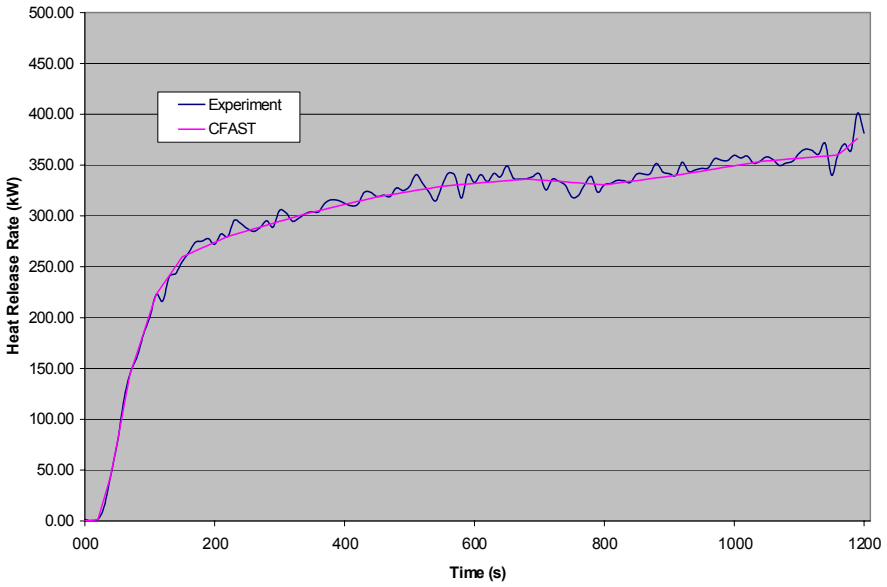

Figure 1 Heat Release Rate (CFAST) - Test 4

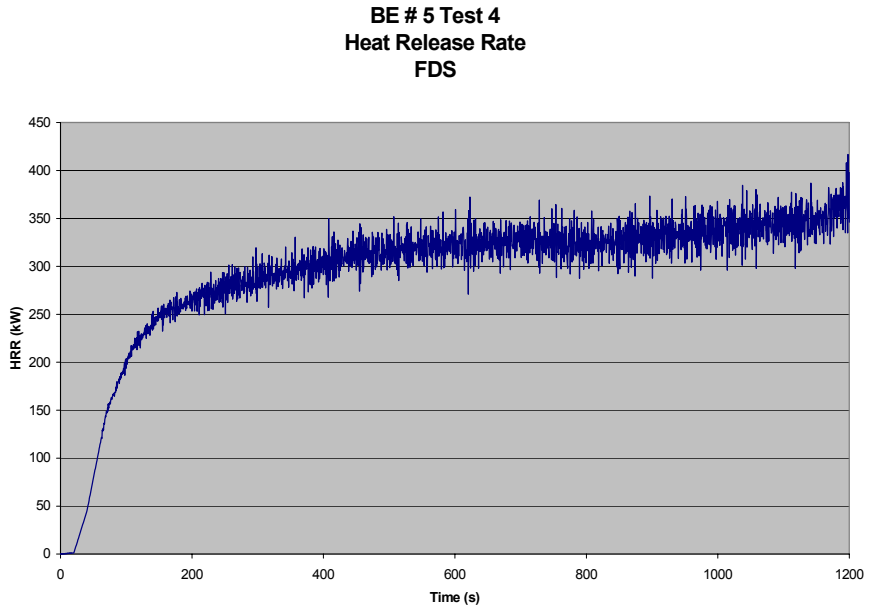

Figure 2 Heat Release Rate (FDS) - Test 4

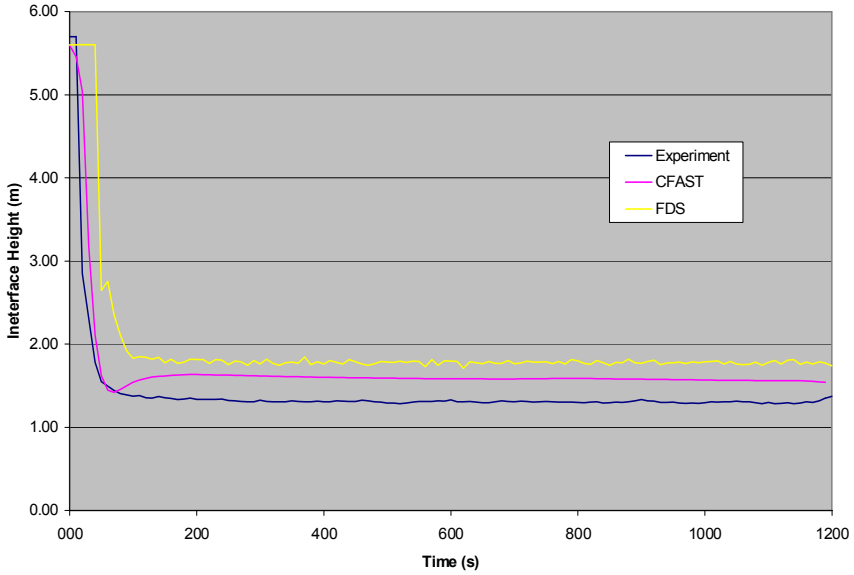

Figure 3 HGL Interface Height - Test 4

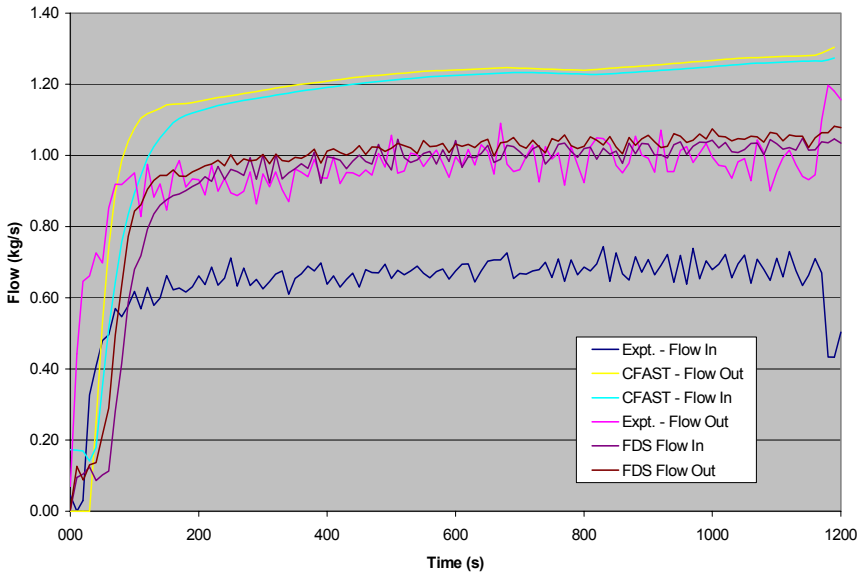

Figure 4 - Door Flows - Test 4

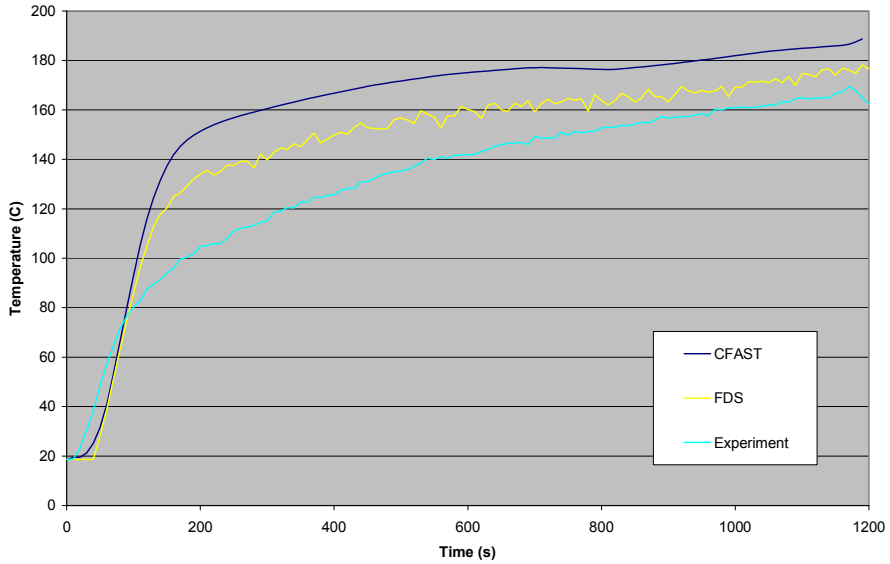

Figure 5 HGL Temperature - Test 4

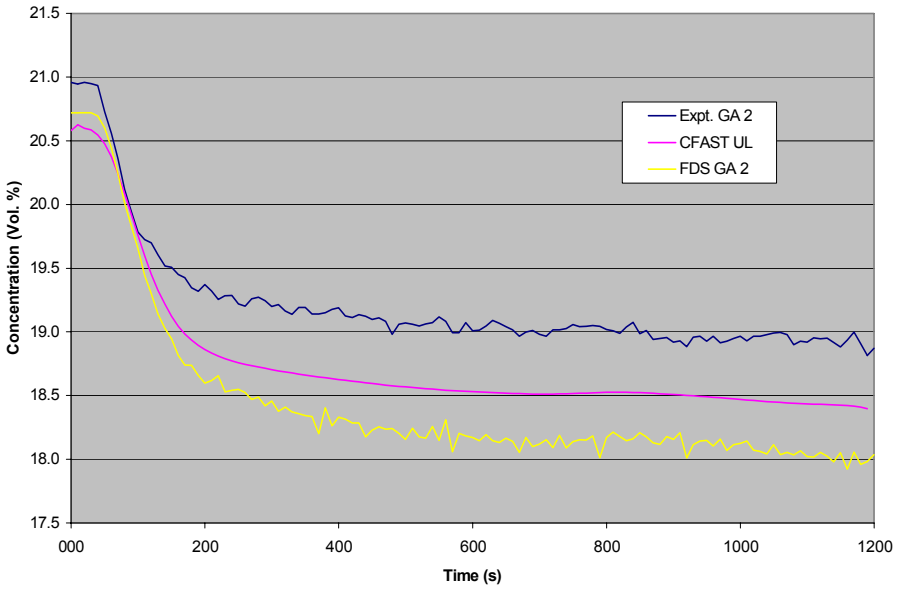

Figure 6 Oxygen Concentration - Test 4

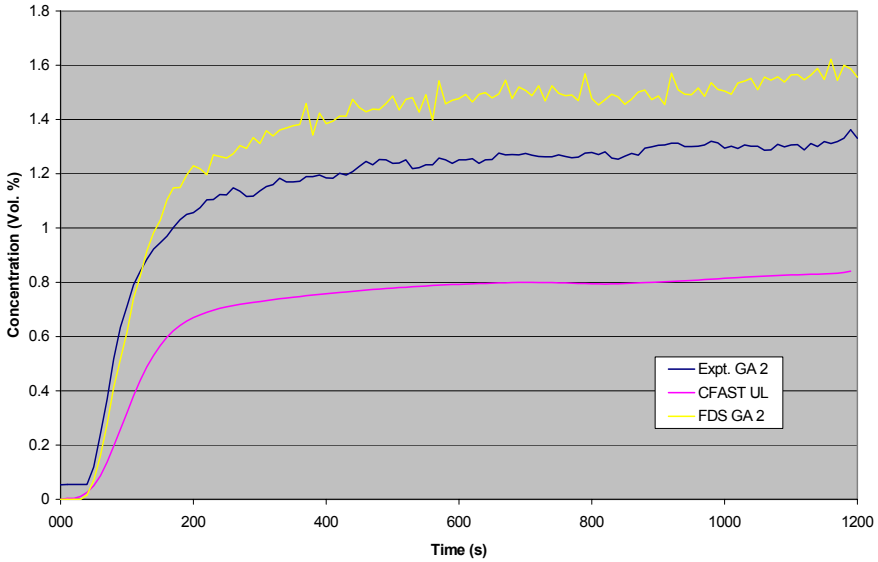

Figure 7 CO2 Concentration - Test 4

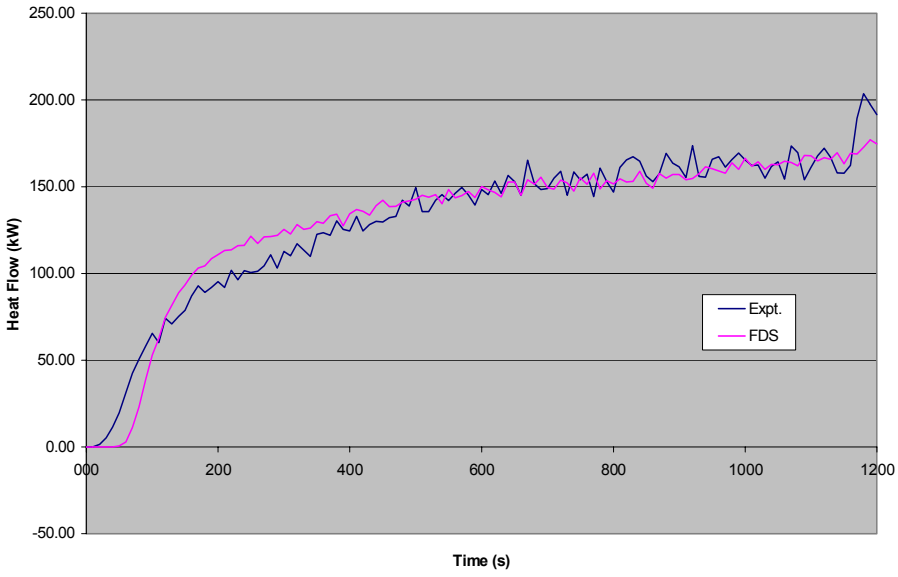

Figure 8 Heat Flow through Door - Test 4

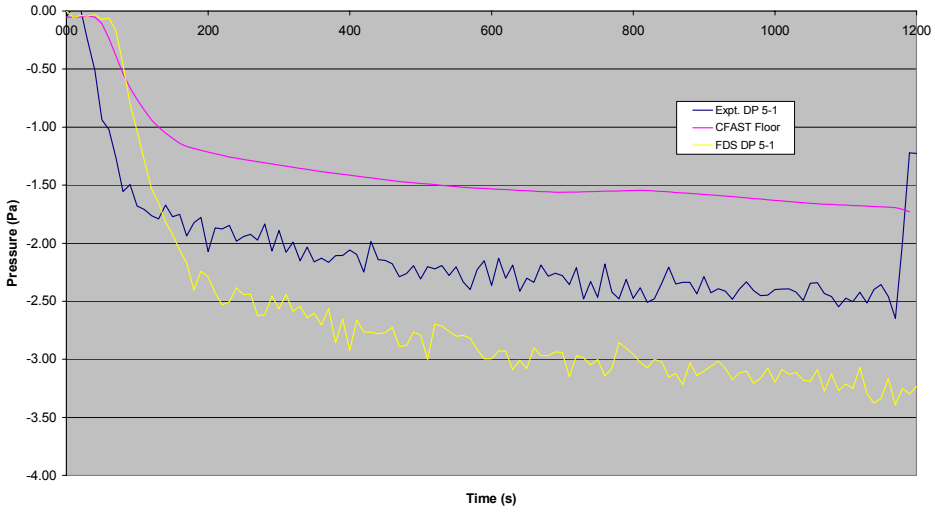

Figure 9 Compartment Pressure - Test 4

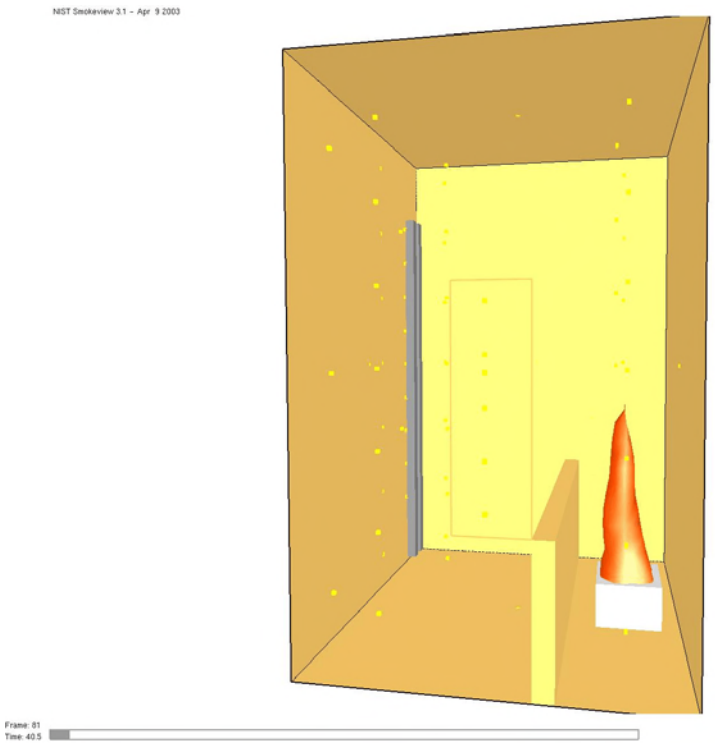

Figure 10 Isosurface of Flame Sheet (40 s) - Test 4

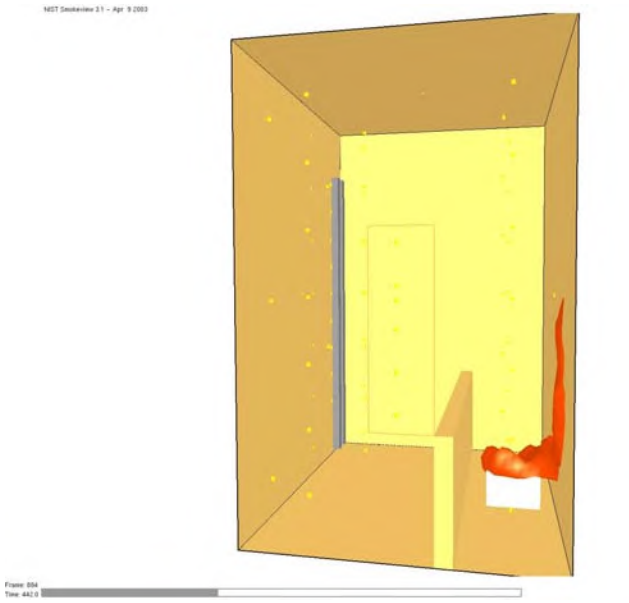

Figure 11 Isosurface of Flame Sheet (442 s) - Test 4

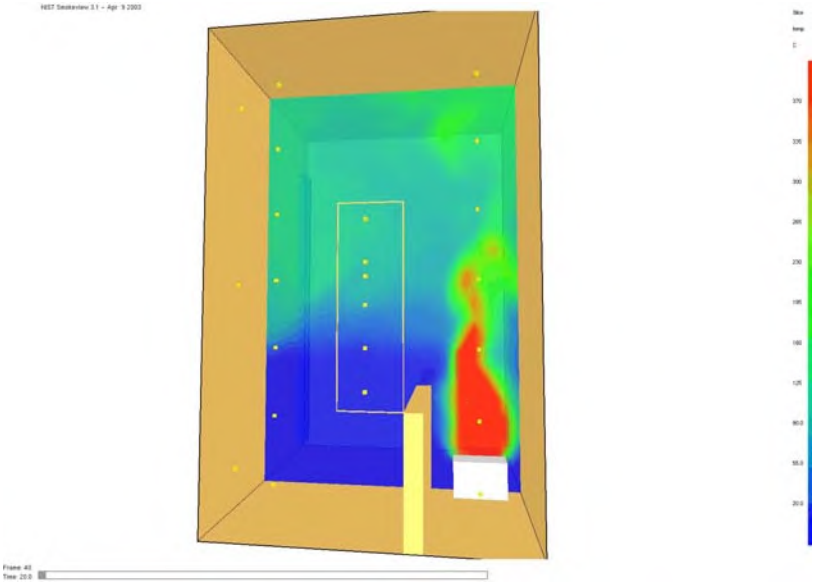

Figure 12 Temperature Slice View (y=1.8 m, 20 s) - Test 4

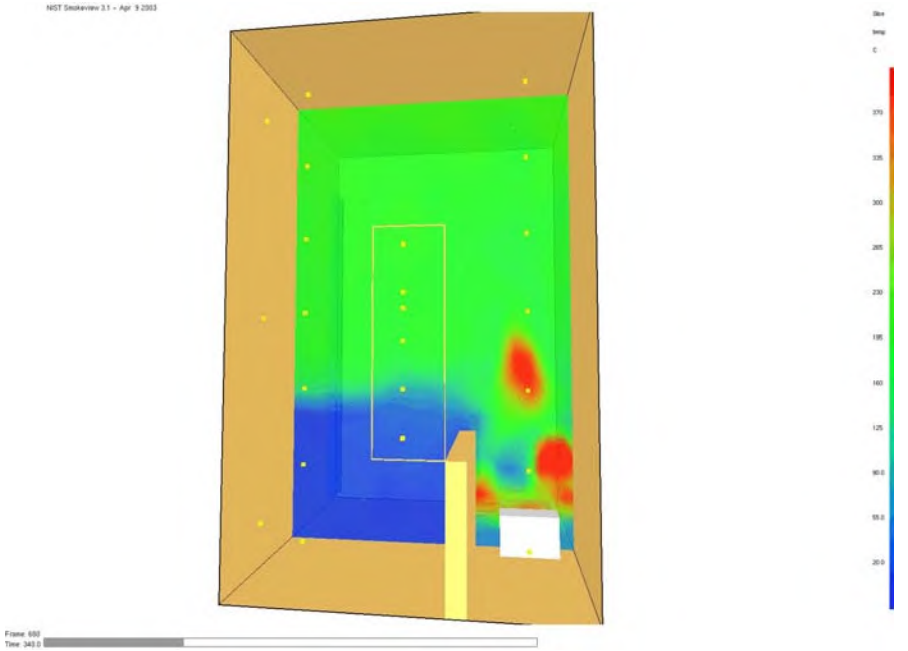

Figure 13 Temperature Slice View (y=1.8 m, 340 s) - Test 4

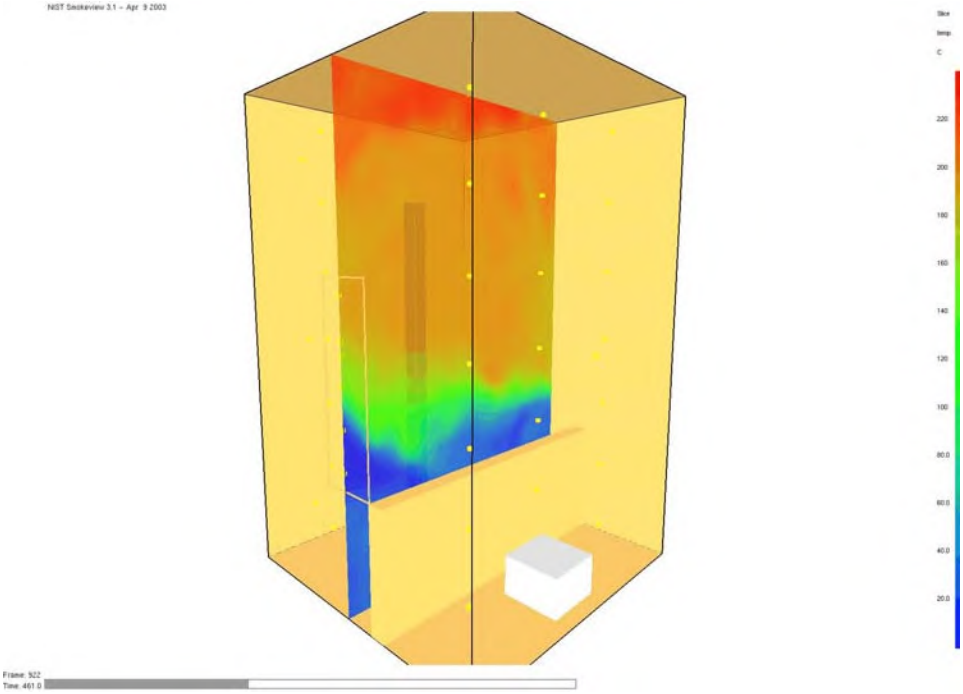

Figure 14 Temperature Slice View (x=1.8 m, 461 s) - Test 4

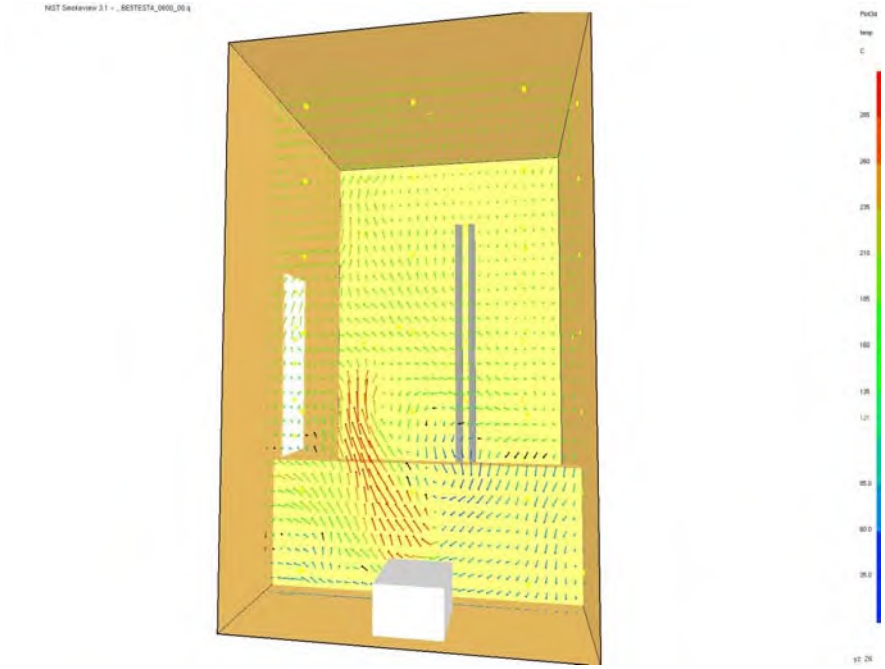

Figure 15 Flow Vectors in Trench (600 s) - Test 4

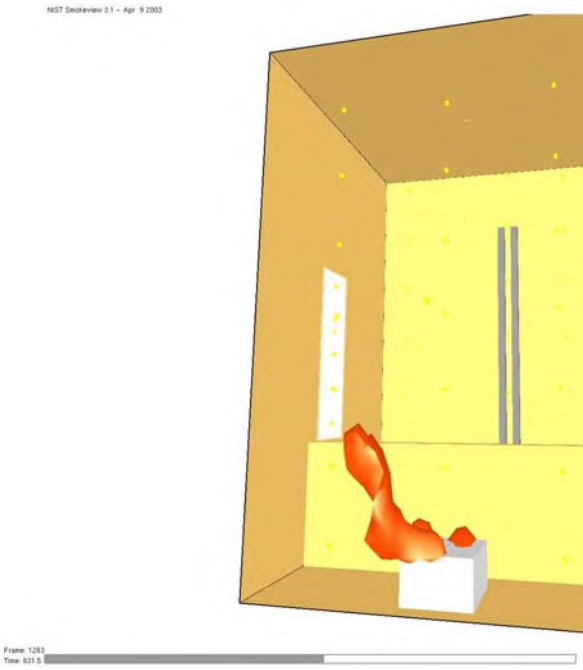

Figure 16 Isosurface of Flame Sheet (631 s) - Test 4

Figure 17 Photograph of Pool Fire in Trench

Figure 18 Photograph of Pool Fire in Trench

Figure 19 Photograph of Pool Fire in Trench

Figure 20 Photograph of Pool Fire in Trench

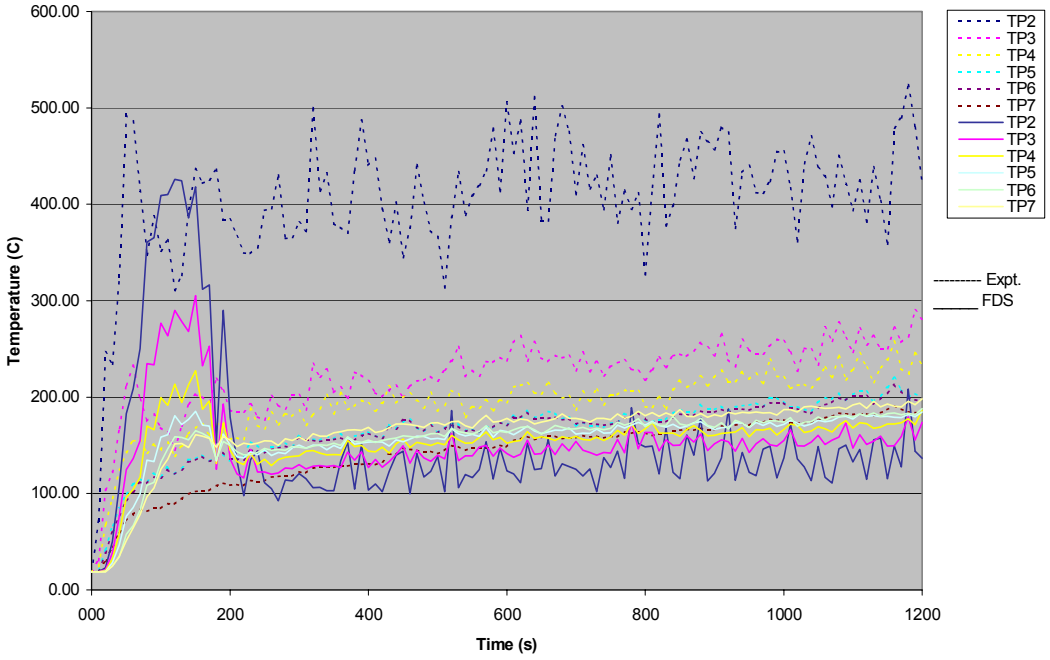

Figure 21 Plume Temperature - Test 4

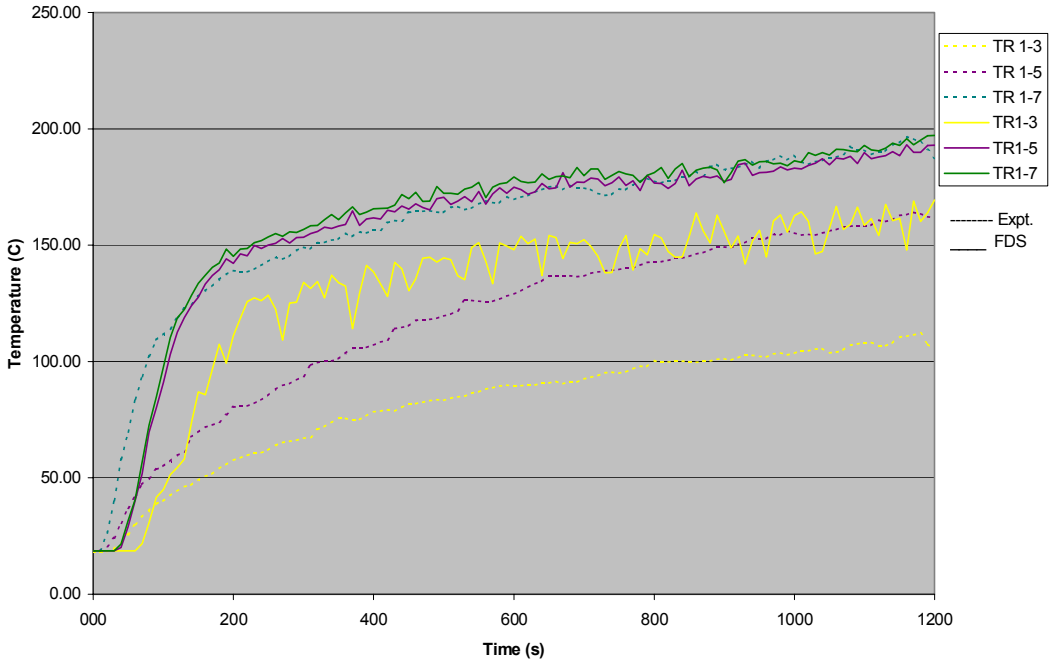

Figure 22 Compartment Temperature (TR1) - Test 4

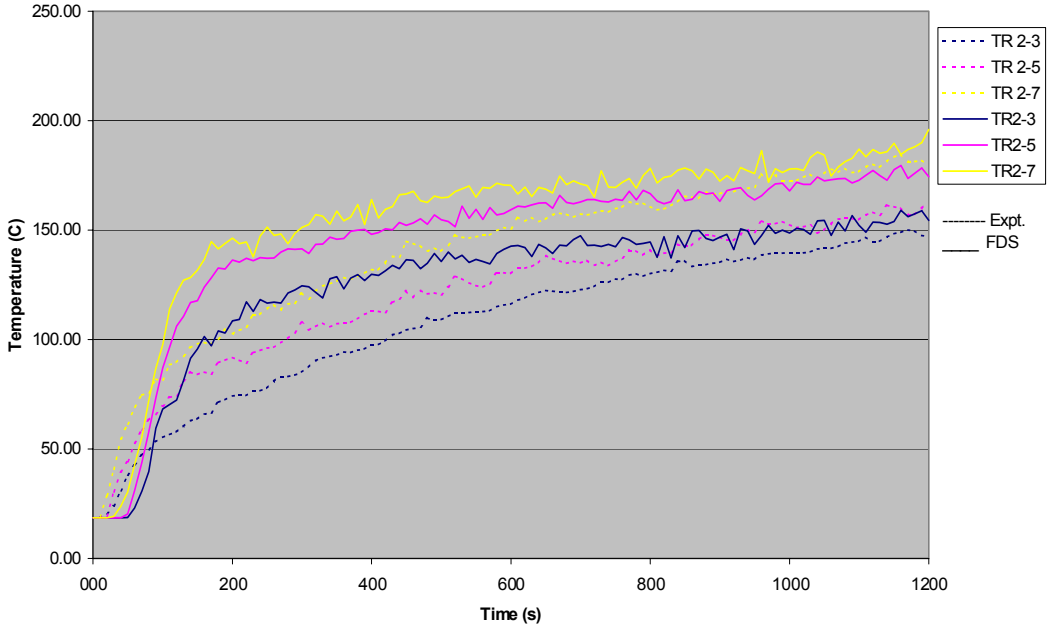

Figure 23 Compartment temperature (TR2) - Test 4

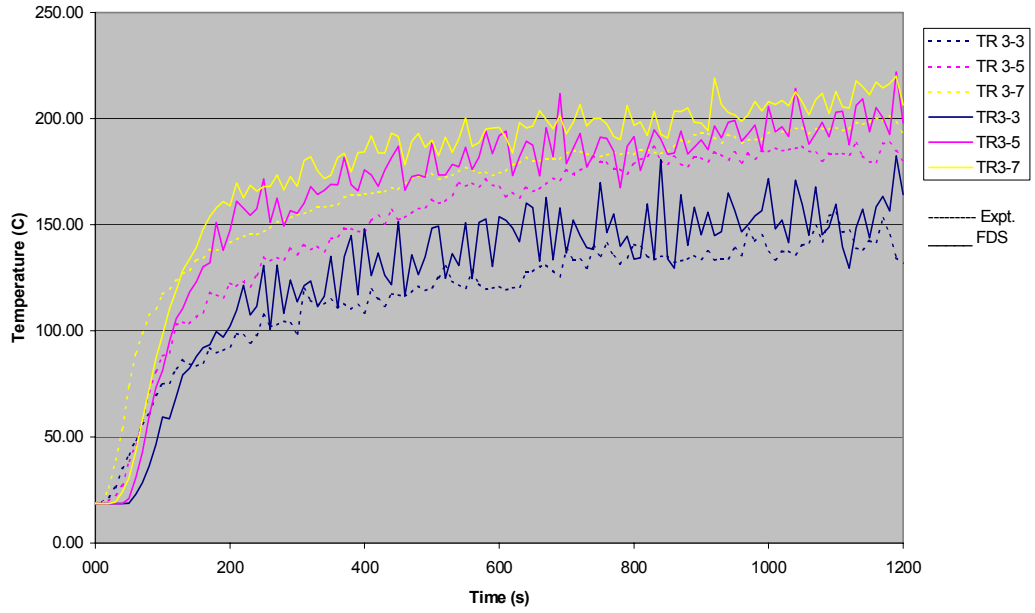

Figure 24 Compartment Temperature (TR3) - Test 4

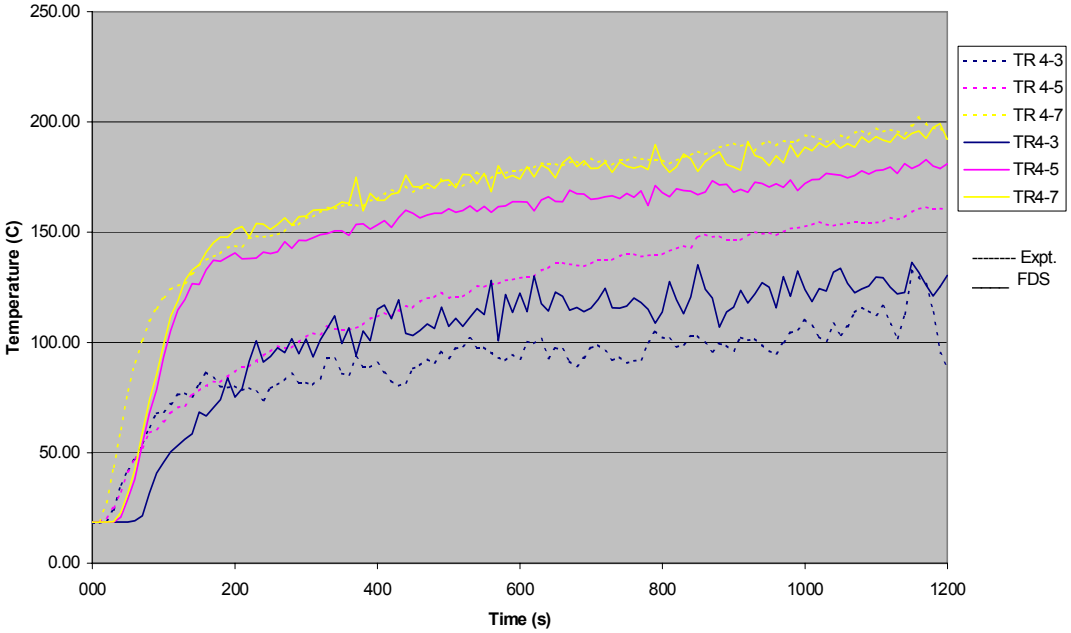

Figure 25 Compartment Temperature (TR4) - Test 4

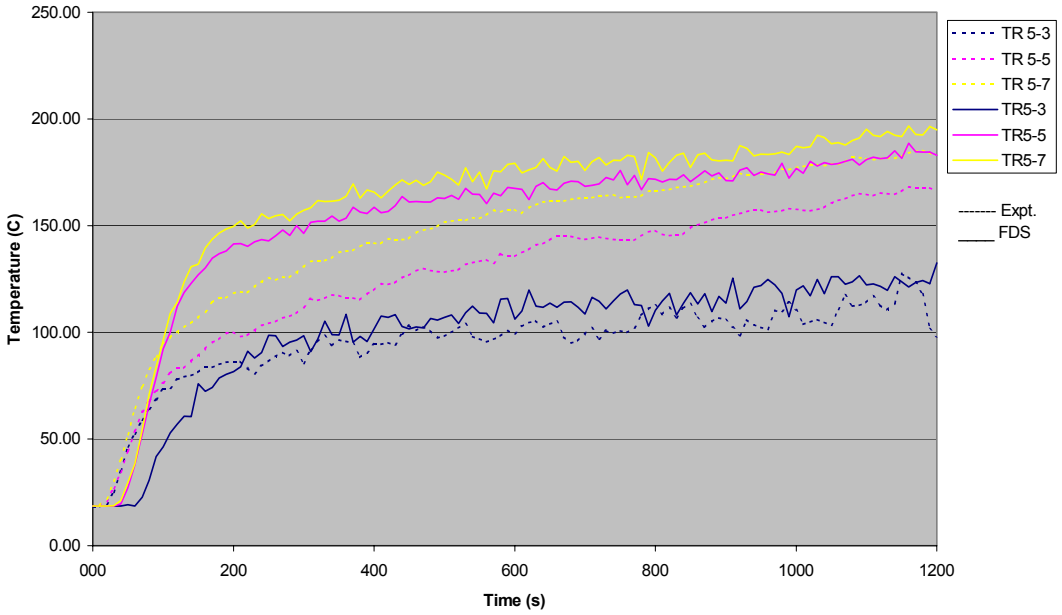

Figure 26 Compartment Temperature (TR5) - Test 4

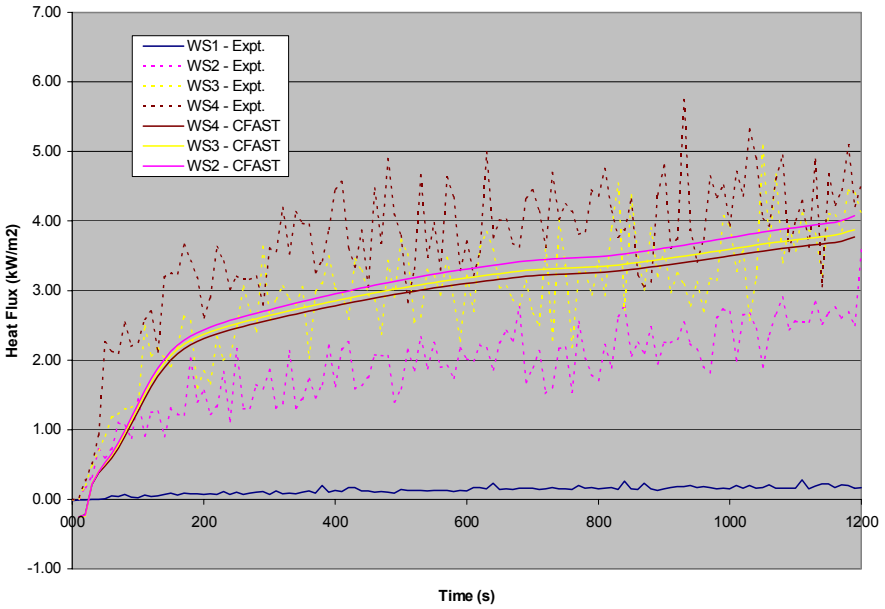

Figure 27 Heat Flux on Cables (CFAST) - Test 4

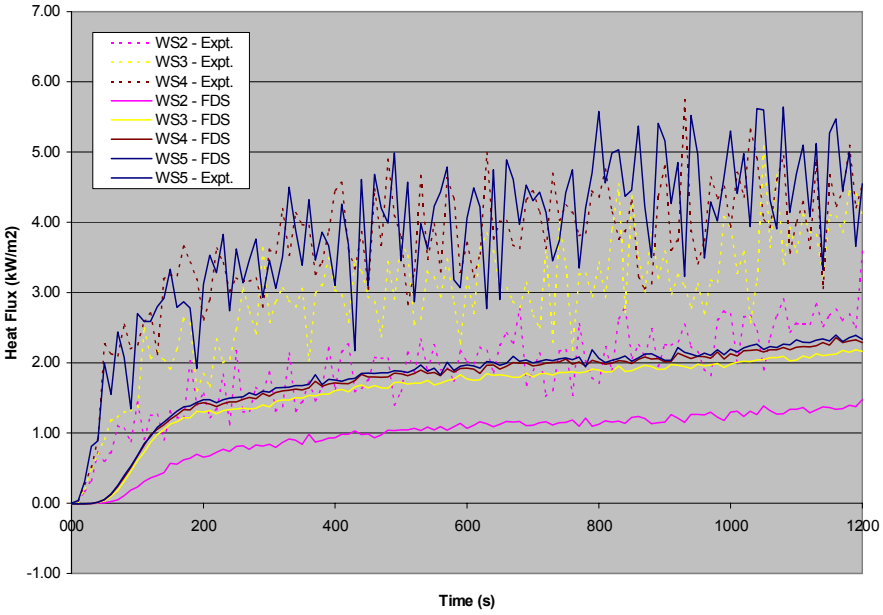

Figure 28 Heat Flux on Cables (FDS) - Test 4

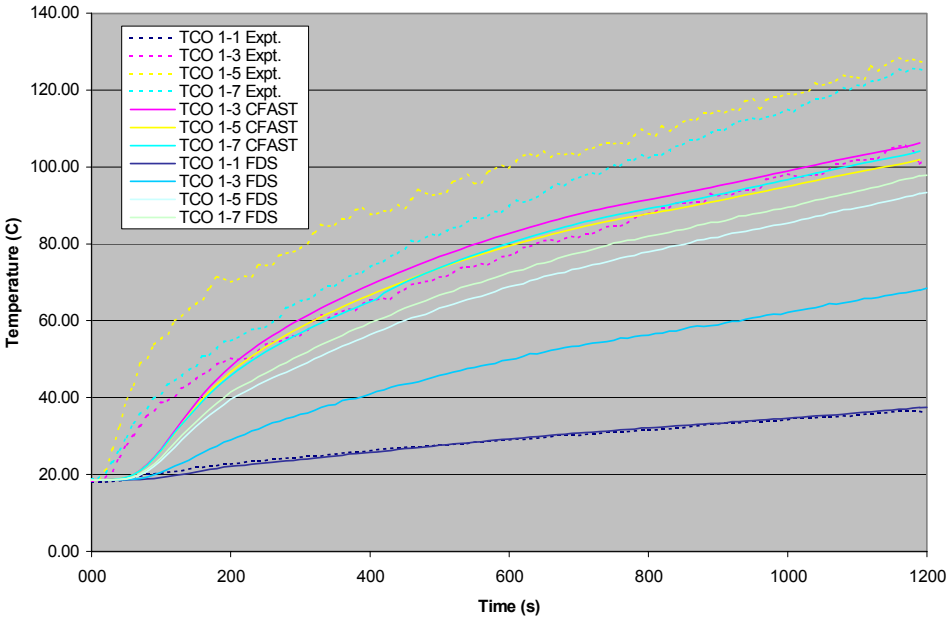

Figure 29 Power Cable Temperature - Test 4

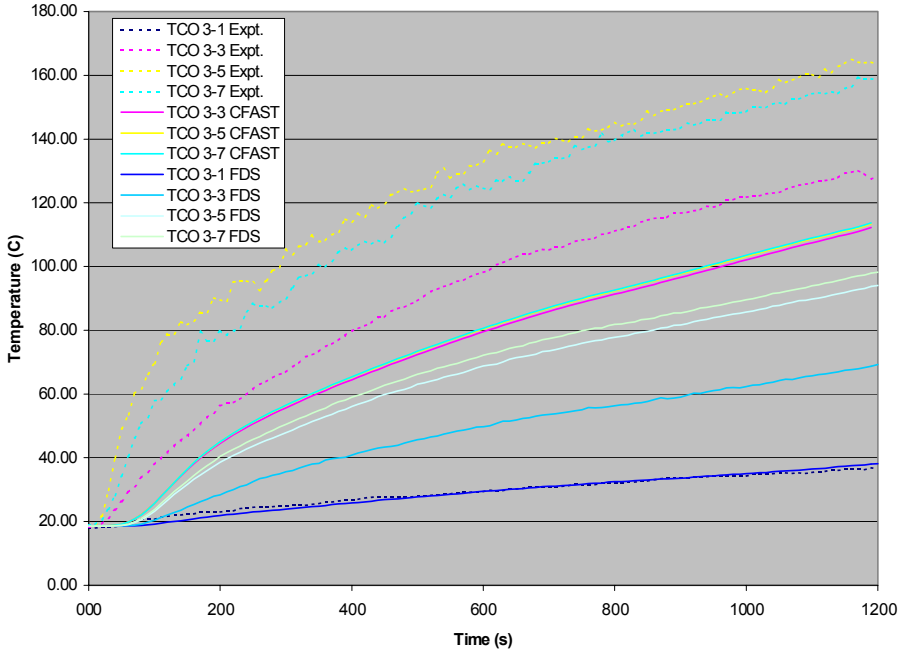

Figure 30 I&C Cable Temperature - Test 4

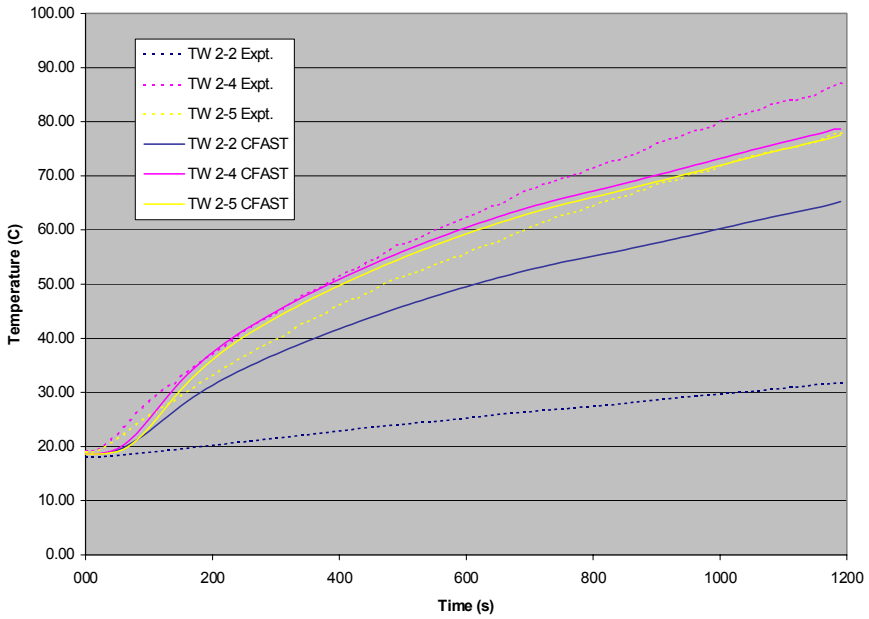

Figure 31 Wall Temperature (TW2-CFAST) - Test 4

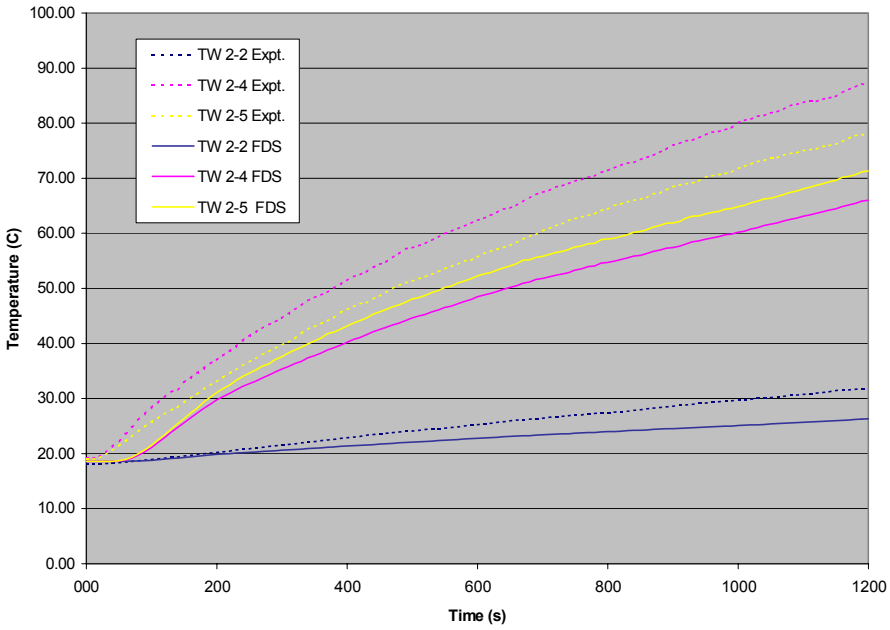

Figure 32 Wall Temperature - (TW2-FDS) - Test 4

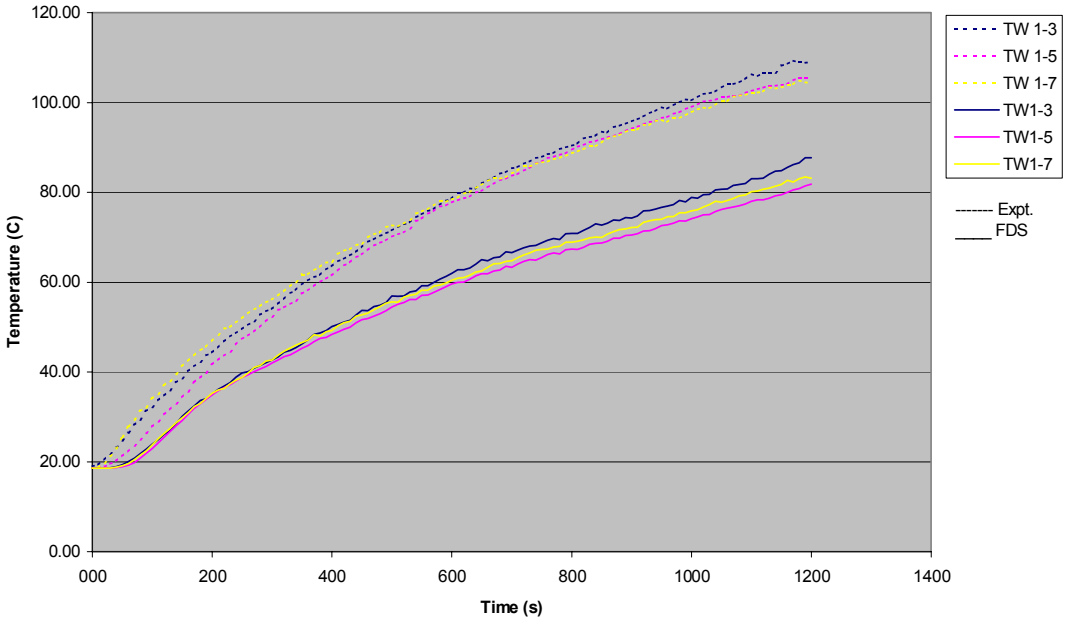

Figure 33 Wall Temperature (TW1) - Test 4

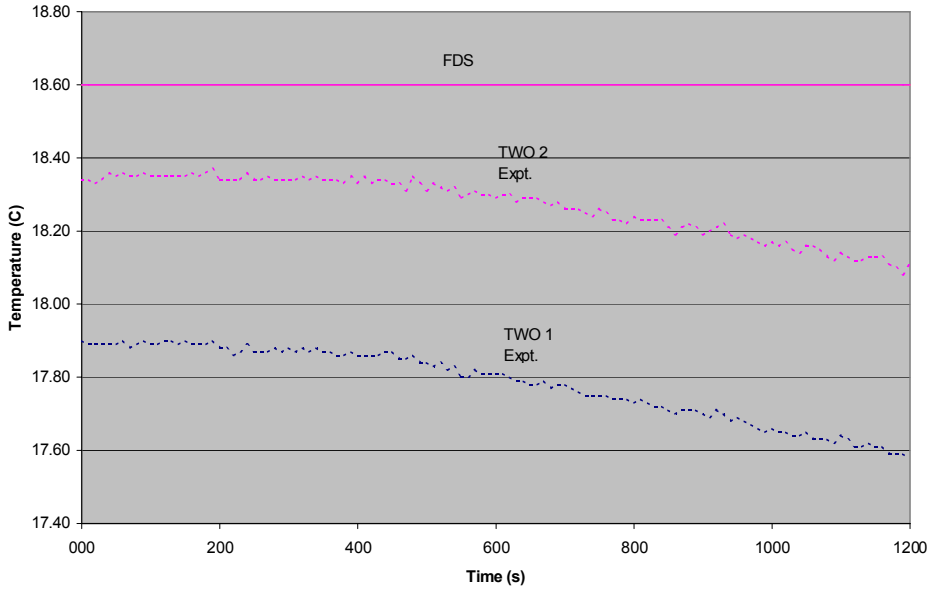

Figure 34 Outside Wall Temperature - Test 4

Appendix A Specification of Benchmark Exercise # 5

(Prepared by iBMB)

Appendix B Input Data for CFAST and FDS

Deytec, Inc.

Nuclear Engineering Services